# Mechanical spectral hole burning of an entangled polymer solution in the stress-controlled domain

Zhiyuan Qian and Gregory B. McKenna[*]

*Department of Chemical Engineering, Texas Tech University, Lubbock, Texas 79409, USA*

Nonresonant spectral hole burning has proven to be a versatile method to characterize the dynamics of complex fluids, including polymers. Early work focused on dielectric susceptibility measurements in glass forming liquids, while recent work from our lab used mechanical viscoelastic measurements to investigate polymer melts and solutions. While the observed results were similar, the interpretations were different, with the former being interpreted by attributing the "holes" in the response as being due to dynamic heterogeneity in the system that is related to the glass or other transition, while the latter was interpreted in a way that suggested that the observed holes depend on the type of dynamics (Rouse, terminal, etc.) rather than an identifiable spatial heterogeneity. In this work, we have expanded mechanical spectral hole burning (MSHB) into the stress-controlled domain and carried out experiments in the rubbery regime of a polystyrene solution, similar to one which was tested previously with strain-controlled MSHB. The effects of pump stress amplitude, pump frequency, and waiting time were investigated. The mechanical holes in both directions (vertical and horizontal) were successfully burned, unlike the strain-controlled MSHB experiments on the same polystyrene solution, in which vertical holes were at best incomplete. The hole intensity exhibits a linear relationship with the amount of energy dissipated in the system during the large mechanical pump modification. The results suggest that the stress-controlled MSHB can be combined with strain-controlled MSHB to build a more complete framework to investigate the dynamics of polymeric materials and is consistent with the dynamic heterogeneity being related to the type of dynamics rather than to localized heating effects.

## I. INTRODUCTION

The dynamics of glass formers (including supercooled liquids and polymers) at the macroscopic scale can be described by a nonexponential relaxation function, such as the Kohlrausch-Williams-Watts (KWW) [1,2] stretched exponential, and can be attributed to two distinct scenarios: homogeneous and heterogeneous [3]. For homogeneous dynamics, all local subensembles exhibit the same dynamics as does the macroscopic system, while for heterogeneous dynamics, each local subensemble has a specific intrinsic response and the overall response of the subensembles yields the macroscopic dynamics. These two scenarios are indistinguishable in the linear response region. Nonresonant spectral hole burning (NSHB) [4] has been proposed to investigate the dynamic heterogeneity, in other words, to differentiate these two scenarios. NSHB has been used to investigate dynamic heterogeneity of small molecule glass formers by dielectric spectroscopy as well as a spin glass by magnetic field spectroscopy near the relevant glass transition temperatures $T_g$ [4–12] or far below $T_g$ and near to the $\beta$ transition [13]. At the same time, dielectric NSHB has been carried out on polar disordered crystals [14–16], and dynamic heterogeneity was observed. In hole burning spectroscopy, the material is subjected to a large sinusoidal pump followed by a small-step probe. Evidence of dynamic heterogeneity is obtained when the large pump "burns" holes (see below), due to a selective modification of the local

dynamics. If the large pump modifies the dynamic response uniformly, it is taken as evidence of dynamic homogeneity [17]. The dynamic heterogeneity (or burned holes) has been related to thermal energy absorbed in selected regions due to the imposed large pump, resulting in local heating and changes in local temperature or its distribution [4–7,17,18].

In the case of polymeric materials, which have low dielectric or magnetic responses, an alternative technique, i.e., mechanical spectral hole burning (MSHB), was developed by Shi and McKenna [19], which is analogous to NSHB. Several different polymeric systems (polymer melts [19,20], polymer solutions [20–22], and a block copolymer [23]) have been thoroughly investigated using MSHB at temperatures well above $T_g$. Evidence of dynamic heterogeneity has been observed in a low density polyethylene melt [19,20] and an poly(styrene-b-isoprene(1,4 addition)-b-styrene) (SIS) triblock copolymer in the ordered state [23]. Qin *et al.* [21] examined a series of polystyrene solutions and found that the observation of holes was related to the type of dynamic regime: Rouse, rubbery, rubbery to terminal, and terminal, rather than to specific length scales related to, e.g., entanglement density or chain end density of the series of solutions investigated. Mechanical holes were observed in the first three regimes but not in the terminal regime. These results were interpreted to imply that dynamic heterogeneity is not necessarily the result of a specific spatial heterogeneity as introduced by changing molecular weight and concentration of the solutions [17]. (While the prior results from MSHB were performed well above the system glass transition temperature, it is worth noting here that a study [24] of dynamic heterogeneity using single molecular

─────────
[*]Corresponding author: greg.mckenna@ttu.edu

fluorescence microscopy on a poly(*n*-butyl methacrylate) thin film resulted in the homogeneity being restored at approximately 19 K above its Differential Scanning Calorimetry (DSC) $T_g$.) Furthermore, the Kaye-Bernstein, Kearsley, Zapas (K-BKZ) nonlinear constitutive model [25,26], into which phenomenologically the simplest form of the Doi-Edwards model falls [27–31], as well as the Bernstein-Shokooh stress clock model [32,33], fail to capture the features of mechanical holes. As shown by Shi and McKenna [19], at best only softening is observed. In addition, Shamim and McKenna [22] have demonstrated that MSHB can provide additional information to the current "fingerprinting" framework [34] of large amplitude oscillatory shear (LAOS) measurements. In the prior MSHB work, the studies were all performed with a strain-controlled rheometer, hence in modulus space. The original dielectric NSHB experiments examined the dielectric susceptibility; hence they were performed in retardation space [4,5], which is equivalent to creep measurements in the viscoelastic regime. Later experiments also included work in relaxation or modulus space [7,9,11–13]. Therefore, it is of interest to expand the current strain-controlled MSHB into stress-controlled conditions and to compare the results with those obtained using strain-controlled experiments. In the current work, we report results from experiments carried out using a stress-controlled rheometer and compare the results with strain-controlled MSHB experiments on a similar polystyrene solution [21,22].

## II. EXPERIMENT

### A. Materials

The polymer solution investigated in this work is a polystyrene (PS)-diethyl phthalate (DEP) solution. The linear PS was purchased from Polymer Source with number average molecular weight ($M_n$) of 980 000 g/mol and polydispersity index (PDI) of 1.16, close to one of the PS-DEP systems studied by Qin *et al.* [21]. The DEP (purity 99.5%) was purchased from Sigma-Aldrich. A 10% mass concentration (wt %) PS-DEP solution (10% PS-DEP) was prepared following the same methods as described in the work of Qin *et al.* [21] and Shamim and McKenna [22]. Toluene was added into the solution as the cosolvent to accelerate the mixing. The concentration of the solution was calculated by the mass of the PS and DEP added into the system prior to evaporation of the cosolvent.

Based on Fox's equation [35] $\frac{1}{T_g} = \frac{w_1}{T_{g,1}} + \frac{w_1}{T_{g,2}}$, the glass transition temperature $T_g$ of the 10% PS-DEP solution is estimated to be $-83\,°C$ if the $T_g$ of the DEP is 180 K [36]. This is $43\,°C$ below the test temperature in the present study.

### B. Methods

The linear viscoelastic response of the solution was obtained by performing dynamic frequency sweeps using an ARES (TA Instruments) rheometer with a cone and plate fixture of 50 mm diameter and 0.0402-rad (2.3°) cone angle and 45.7-$\mu$m truncation gap over the temperature range of $-40\,°C-0\,°C$ using a liquid nitrogen cooling system. A master curve was constructed using time-temperature superposition [37] to establish the dynamic regime in which the hole burning experiments were performed.
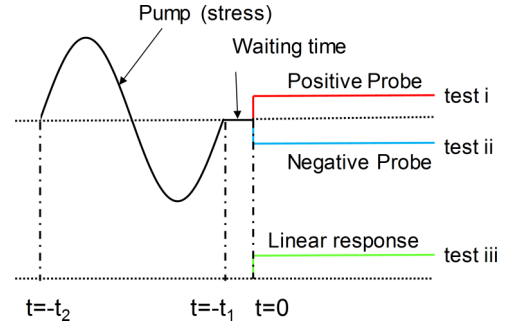


FIG. 1. Schematic of stress-controlled mechanical spectral hole burning (stress_MSHB) experiments.

The stress-controlled mechanical spectral hole burning (stress_MSHB) experiments were carried out on a stress-controlled rheometer MCR 501 (Anton Paar GmbH) with RHEOCOMPASS™ software. A 25-mm-diameter cone and plate fixture (1° cone angle (0.0175 rad), and 50-$\mu$m truncation gap) with TRUGAP™ function was used. The instrument is equipped with a CTD 600 oven with a TC 30 temperature controller for temperature control. The temperature was stable within $\pm 0.2\,°C$. Liquid nitrogen was used as the cooling source for low temperature measurements. Dynamic amplitude sweep tests and creep tests were performed to determine the linear and nonlinear stress regimes at $-40\,°C$. The stress_MSHB tests were performed at $-40\,°C$ (which is approximately $43\,°C$ above the $T_g$ of the 10% PS-DEP solution) with pump frequency ranging from 0.02 to 0.1 Hz, pump stress amplitudes from 2000 to 3000 Pa, and probe amplitude of 25 Pa.

Analogous to the strain-controlled MSHB (strain_MSHB), the stress-controlled MSHB experiment consists of three separate tests, which are shown schematically in Fig. 1. In the first two tests, one cycle of a large amplitude sinusoidal stress in the nonlinear regime (referred to as the "pump") is applied to the sample. This is followed by a small positive or negative step stress, referred to as the "probe." The resulting creep compliances from these two tests can be described as

$$J_+(\omega, \sigma, t) = J_{\text{pump}}(\omega, \sigma, t) + J_{\text{mod}}(\omega, \sigma, t),$$
$$J_-(\omega, \sigma, t) = J_{\text{pump}}(\omega, \sigma, t) - J_{\text{mod}}(\omega, \sigma, t).$$

By applying a phase cycling procedure, the "aftereffect" [4] caused by the sinusoidal pump stress input is removed, and the modified creep response $J_{\text{mod}}(\omega, \sigma, t)$ is obtained, which is written as follows:

$$J_{\text{mod}}(\omega, \sigma, t) = \frac{J_+(\omega, \sigma, t) - J_-(\omega, \sigma, t)}{2}.$$

In the third separate test, the sample is only subjected to the same linear step stress performed in the first two tests; i.e., the linear (unmodified) creep compliance $J_{\text{linear}}(t)$ is obtained. $J_{\text{mod}}(\omega, \sigma, t)$ and $J_{\text{linear}}(t)$ are plotted against the logarithm of the probe time in Fig. 2 and this provides a comparison between $J_{\text{linear}}(\omega, \sigma, t)$ and $J_{\text{mod}}(\omega, \sigma, t)$. As depicted in the inset, the mechanical vertical and horizontal spectral modifications (spectral holes) are defined as differences between the linear and modified compliance $|\Delta J(\omega, \sigma, t)|$ at the same time, and the logarithmic time difference $|\Delta \log(t)|$ at the same compliance level, respectively. A cubic spline curve
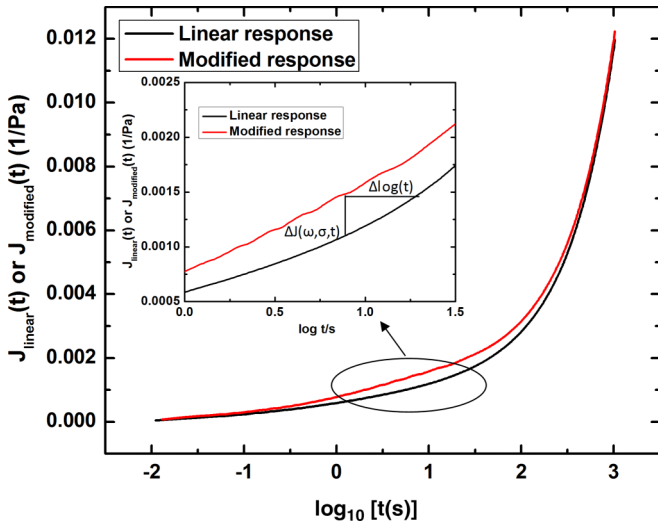
FIG. 2. Example of vertical and horizontal spectral modifications (spectral holes) obtained from the difference between linear response and modified response in the vertical and horizontal directions.

fitting algorithm available in MATLAB was used to perform the interpolation required to calculate the vertical and horizontal differences.

Between tests, a sufficient time [$\geqslant$45 min, which is approximately 27 times the relaxation time ($\sim$100 s) obtained from the crossover point in Fig. 3] was taken to allow the sample to relax back to the initial equilibrium state. This was confirmed by the well overlapped strain response curves for the large amplitude sine wave (pump) in the experiment and that imposed after the completion of the hole burning series of tests to assure reproducibility.

## III. RESULTS AND DISCUSSION

The dynamic modulus [$G'(\omega)$ and $G''(\omega)$] master curves for the 10% PS-DEP solution at a reference temperature of
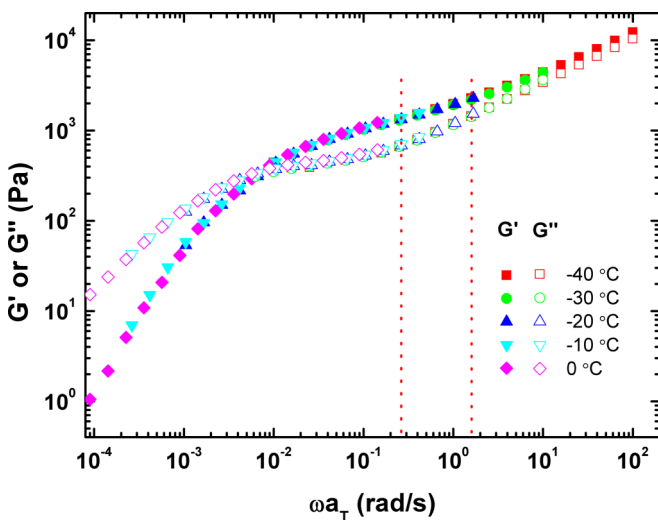


FIG. 3. Master curve of 10% PS-DEP solution at a reference temperature of $-40\,^\circ$C. The red dashed lines show the pump frequency range corresponding to the rubbery plateau regime. The relaxation time obtained from the crossover point is approximately 100 s.
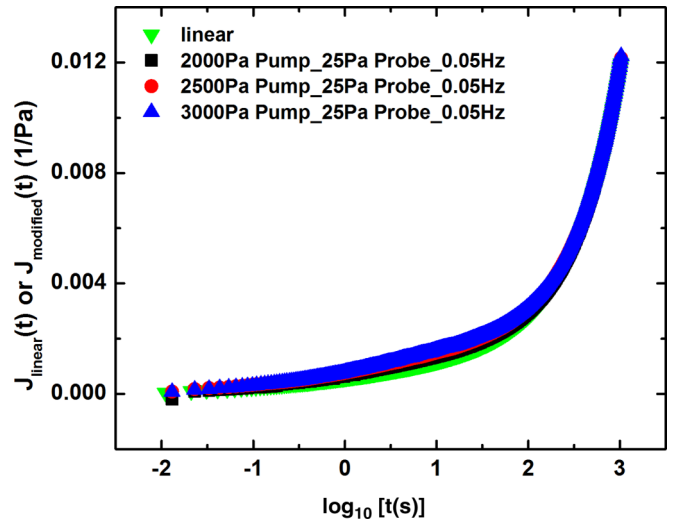


FIG. 4. The linear and modified creep compliances of 10% PS-DEP solution at $-40\,^\circ$C at different pump stress amplitudes: 2000, 2500, and 3000 Pa. The pump stress frequency is 0.05 Hz and the probe stress is 25 Pa.

$-40\,^\circ$C are shown in Fig. 3. The red dashed lines indicate the range of pump frequency used for our stress-controlled MSHB tests, which is in the rubbery plateau regime of the system.

The stress_MSHB experiments on the 10% PS-DEP solution were performed in the same dynamic regime as the strain_MSHB experiments (performed previously by Qin *et al.* [21], and Shamim and McKenna [22]), i.e., the rubbery plateau region for the frequency range of 0.02–0.1 Hz at $-40\,^\circ$C. The effects of pump stress amplitude, pump frequency, and waiting time between pump and probe on the vertical holes and horizontal holes were investigated and are compared with the prior strain_MSHB results.

### A. Pump stress amplitude effect

The first effect discussed here is the pump amplitude effect, where the pump stress amplitude (in the nonlinear region) was varied from 2000 to 3000 Pa; the pump frequency and probe stress were fixed at 0.05 Hz and 25 Pa, respectively; and no waiting time was applied between the pump and the probe. Figure 4 shows the obtained linear and modified creep compliances. It is readily seen that the curves do not overlap onto each other.

The mechanical spectral modifications in the vertical direction (vertical holes) and horizontal direction (horizontal holes) were calculated and are shown in Fig. 5. The presence of vertical and horizontal holes (the peaks) for all three pump amplitudes indicates the presence of dynamic heterogeneity in the rubbery plateau region. For the horizontal holes, similar to the results from strain_MSHB of a similar molecular weight 10% PS-DEP solution [21,22], both hole intensity and position are pump amplitude dependent; i.e., the hole intensity increases with the pump stress amplitude and the peak position shifts to longer time. For the vertical holes, in contrast to strain_MSHB, in which only shoulderlike or incomplete vertical holes were obtained [21,22], the current stress_MSHB gives complete vertical holes (first peak in the plot). While the hole intensity
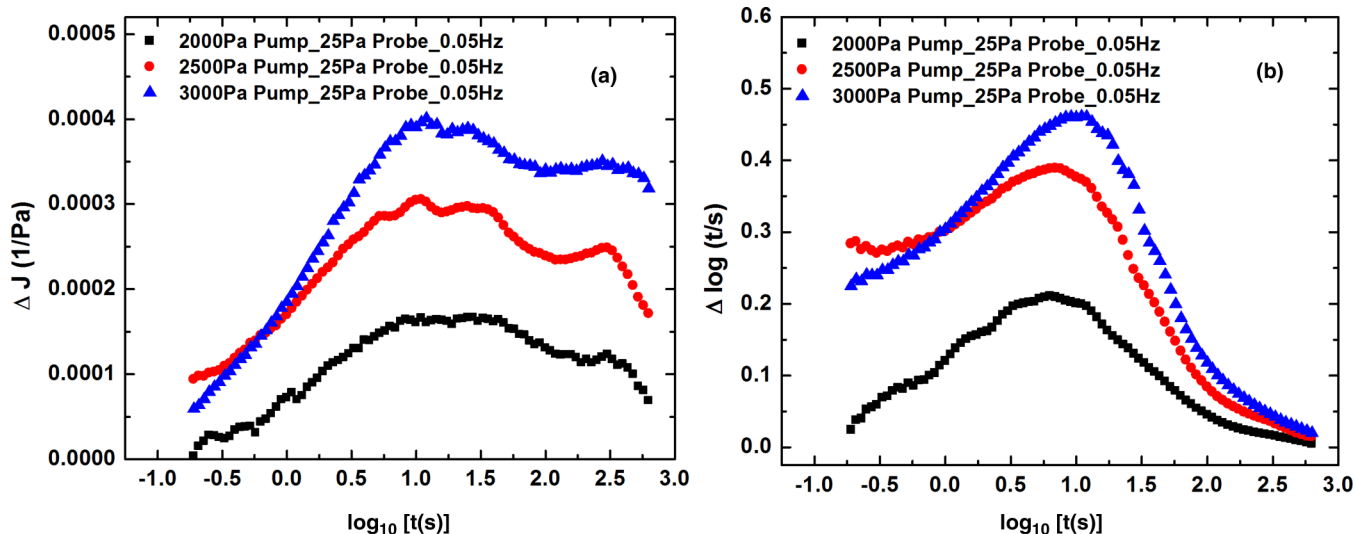
FIG. 5. The mechanical spectral modifications in (a) vertical direction and (b) horizontal direction for 10% PS-DEP solution at $-40\,°C$ under different pump stress amplitudes: 2000, 2500, and 3000 Pa. The pump stress frequency and probe stress are 0.05 Hz and 25 Pa, respectively. In (a), the first peak refers to the vertical hole; the second peak refers to the long-time peak in the context.

is pump amplitude dependent, i.e., it increases with pump stress amplitude, the hole position on the log time axis is almost independent of pump amplitude. This is different from the horizontal holes. Similar behavior of no change in the vertical hole position with pump amplitude has been reported by Qin *et al.* [21] for other weight concentration PS-DEP solutions, where complete vertical holes were obtained, and by Shamim and McKenna [22] for a polybutadiene-oligomer solution with strain_MSHB. This suggests that the nature of the dynamic heterogeneity does not vary with the pump amplitude. Moreover, the increase in hole intensity with pump amplitude may also be related with the degree of nonlinearity of the system. At a constant pump frequency, the nonlinearity increases with the pump amplitude; i.e., the difference between modified and linear creep responses increases. As a result, the hole intensity increases.

Figure 6 plots hole intensity (vertical hole and horizontal hole) as a function of the square of pump amplitude. Good quadratic dependences are shown for both vertical and horizontal holes. This is consistent with prior findings from other hole burning experiments: strain_MSHB [19–23] and dielectric and magnetic NSHB experiments [4–6,8,10,14–18]. We remark that in the case of dielectric measurements, where the experiments were carried out near $T_g$, such dependence has been attributed to the local heating caused by the energy dissipation during the pump cycle combined with the frequency dependence and breadth of the dynamic heat capacity (related to the heat capacity jump at $T_g$). However, in MSHB, as discussed by Qin *et al.* [21], the polymeric materials were tested at temperatures well above their $T_g$, where the heat capacity is insensitive to temperature and frequency; nevertheless, the quadratic dependence on pump amplitude is observed.
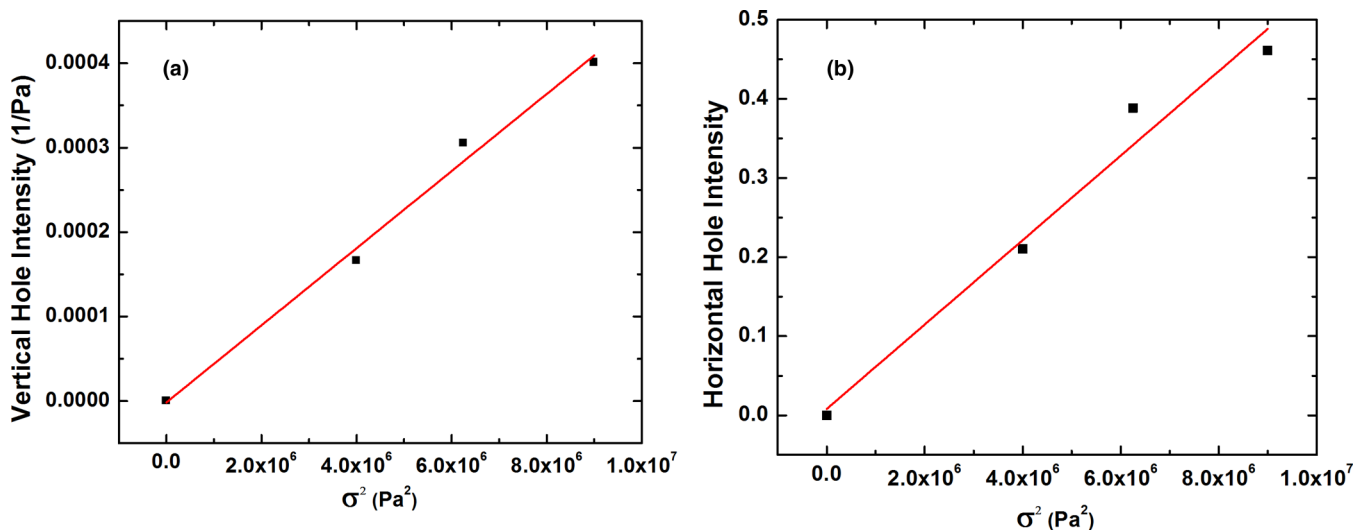


FIG. 6. The hole intensities in (a) vertical direction and (b) horizontal direction as a function of the square of pump stress amplitude.
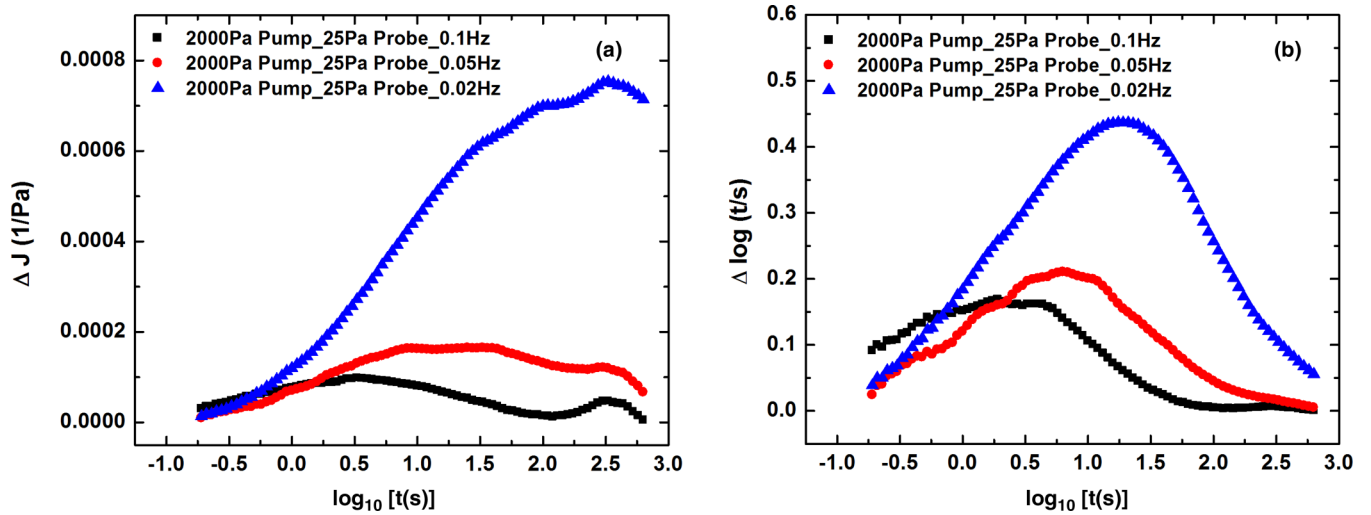
FIG. 7. The mechanical spectral modifications in (a) vertical direction and (b) horizontal direction for 10% PS-DEP solution at $-40\,°C$ under different pump stress frequencies: 0.02, 0.05, and 0.1 Hz. The pump stress amplitude and probe stress are 2000 and 25 Pa, respectively.

It is worth noting that in large amplitude oscillatory shear (LAOS) tests, the normalized third harmonics intensity $I_{3/1}$ also shows a similar quadratic dependence on the pump amplitude; however, the origins of such dependence of the harmonics and burned holes are different. For the harmonics, it can be directly linked to the nonlinear constitutive model, such as the Doi-Edwards model [27–31,38,39]. At this point, the observed holes have not been able to be obtained within a nonlinear constitutive framework such as the K-BKZ [25,26] nonlinear fluid model or the Bernstein-Shokooh [32,33] stress clock model, though the quadratic dependence of the hole intensity is related to the energy dissipation which varies as the square of the pump amplitude as originally postulated by Schiener *et al.* [4].

In addition to the first peak (vertical hole) found in the vertical direction, a second peak located at approximately $\log(t) = 2.5$ can be seen in Fig. 5(a). We refer to this as a long-time peak. Similar to the vertical hole, the intensity of this long-time peak increases with pump amplitude and the peak position remains almost unchanged. We address this long-time peak in the last part of the Discussion section.

### B. Pump frequency effect

The effect of pump frequency on the MSHB response was investigated by varying the frequency: 0.02, 0.05, and 0.1 Hz, at a fixed pump stress amplitude (2000 Pa) and probe stress (25 Pa). The obtained mechanical spectral modifications are plotted in Fig. 7. The vertical and horizontal holes are clearly burned for all three frequencies, consistent with the concept of dynamic heterogeneity in these systems. (Despite the slight wiggling in the curves, the features of the observed hole are not affected. Also, similar wiggling has been observed in some dielectric and magnetic NSHB experiments [4,5,9,10,14,16]). For both vertical and horizontal holes, frequency-dependent hole intensity and position are observed; i.e., the intensities of vertical holes and horizontal holes increase with the decrease of pump frequency and the positions shift to longer time. A similar pump frequency dependence of hole intensity and position has

been reported by Qin *et al.* [21] with strain_MSHB. In their work, such dependence was interpreted by the equivalence between the molecular relaxation time and the timescale of the pump modification. In the rubbery plateau, the majority of molecules in the system have long relaxation times; this responds to the low frequency (long timescale) mechanical pump modification. The same idea can be applied to the current stress_MSHB tests: The mechanical pump of a given frequency selectively modifies the molecules that have equivalent retardation time. Therefore, as the pump frequency decreases, the hole intensity increases. It is worth mentioning here that Qin *et al.* [21] showed in their strain_MSHB work that the frequency dependence of hole intensity varies with the dynamic region; i.e., in the Rouse and rubbery plateau regions, the hole intensity increases with deceasing frequency, while in the rubbery plateau-to-terminal region, it increases with frequency due to relatively faster relaxation (retardation) process in this region. For the hole position, it shifts to longer time as frequency decreases regardless of dynamic regime.

Figure 8 shows the frequency dependence of the positions of the horizontal and vertical holes. Also shown is the position of horizontal hole from strain_MSHB from the work of Qin *et al.* [21] for the same composition 10% PS-DEP solution at $-40\,°C$. We remark that the results of the strain_MSHB of 10% PS-DEP solution show only in complete horizontal holes. In the case of vertical holes in the current stress_MSHB, at the lowest frequency 0.02 Hz, the exact hole position is not clearly defined. Therefore, only 0.05 and 0.1 Hz are considered. It is readily seen that a power-law dependency is achieved in all three cases. The hole position from stress_MSHB gives a similar frequency dependence ($\omega^{-1.36}$ and $\omega^{-1.46}$) for both vertical and horizontal holes, and the dependences are relatively stronger compared with that of the horizontal hole obtained in strain_MSHB measurements in the same rubbery plateau regime ($\omega^{-1.08}$) [21] for the same composition 10% PS-DEP solution. However, the result is close to the observed frequency dependence for the hole position in a 20% PS-DEP solution in the Rouse regime ($\omega^{-1.4}$) [21]. In the case of dielectric NSHB, frequency-dependent hole positions ($\omega^{-\alpha}$)
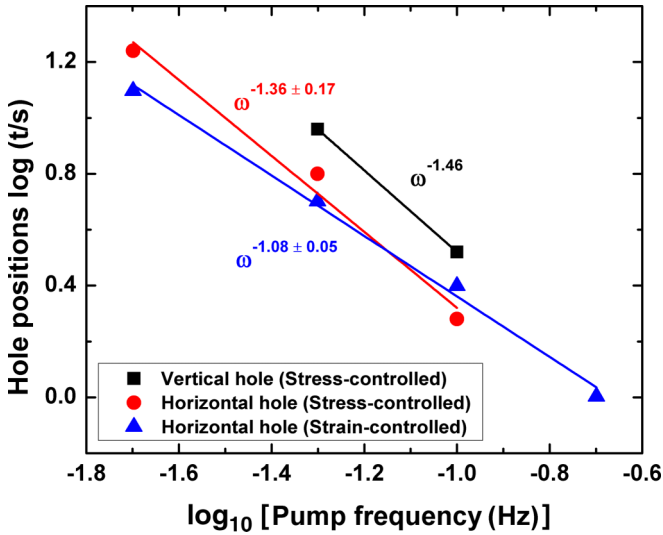
FIG. 8. The frequency-dependent hole position of stress-controlled (current work) and strain-controlled (Qin *et al.* [21]) MSHB of 10% PS-DEP at $-40\,^\circ$C. Uncertainties on the power-law exponents represent standard errors of estimate from the linear fit to the double logarithmic data.

have been observed as well, where $\alpha$ has been reported no greater than unity (ranging from 0.3 to 1.0) for various small molecule glass forming liquids [8,9,11,13–16]. The smaller values of $\alpha$ were interpreted to imply a narrower distribution of relaxation times [11,16]. Hence, the bigger value observed in stress_MSHB would indicate that 10% PS-DEP solution has a broader distribution of retardation times in this interpretation. Also, the observed different frequency dependence may be associated with different dynamic regimes probed in the dielectric and mechanical hole burning experiments; viz., the MSHB work is done well above the glass transition temperature and in the rubbery plateau region while the dielectric measurements have generally been near or below the $T_g$, Thus the origins of the power-law exponents in the MSHB remain an open question. Further work to develop appropriate models for the mechanical hole burning experiments in polymer solutions (and possibly melts) is required to explain this behavior.

### C. Energy dissipation

In the case of dielectric and magnetic NSHB, the experiments have been performed in the vicinity of the $T_g$, where the heat capacity is a strong function of temperature and frequency, though other work has been carried out below the $T_g$ and near a strong $\beta$ relaxation [13]. The presence of holes (vertical and horizontal), i.e., dynamic heterogeneity, has been attributed to localized temperature changes ($\Delta T$) caused by a local heating effect due to the large pump. A $\Delta T$ of 20 mK to as high as 600 mK has been estimated based on the dielectric dissipation in the various materials [11,13,17] and the spectral modifications related to the dependence of the relaxation times on frequency and temperature—strong near the glass transition but weaker near the $\beta$ relaxation. In the case of the work near the $T_g$ the frequency dependence is related to the step change in heat capacity at $T_g$.
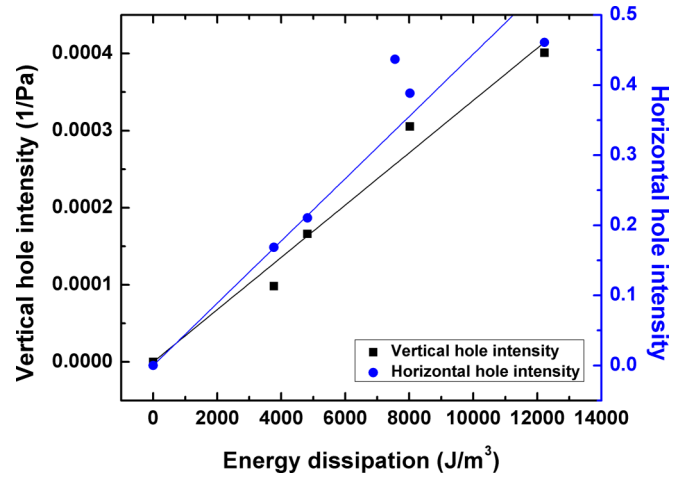


FIG. 9. The intensities of vertical hole (black symbols) and horizontal hole (blue symbols) as functions of energy dissipation per unit volume per cycle for stress_MSHB 10% PS-DEP at $-40\,^\circ$C. (The vertical hole intensity of the measurement with 0.02-Hz pump frequency is not included in the plot since the peak position and intensity are not well defined.)

Similarly, in the current stress_MSHB, the temperature change due to the energy dissipated by the sample during the pump cycle can be estimated. The energy absorption per cycle per unit volume, $W$, is defined as $W = \int_0^{2\pi/\omega} \sigma \dot{\gamma} dt$ [40]. (Note that in the case of a linear response $W = \int_0^{2\pi/\omega} \sigma \dot{\gamma} dt = \pi \gamma_0^2 G''(\omega)$ [40].) Figure 9 plots the hole intensity as a function of energy dissipation. For both vertical and horizontal holes, the intensities are proportional to the energy dissipated by the system. This linear relationship is consistent with the NSHB experiments [4,5,7–11,13–16], as well as with the observation of the quadratic dependence on the applied stress.

Based on the energy dissipation ($W$), the temperature change ($\Delta T$) is defined as $\Delta T = W/(\rho C_p)$, where $\rho$ and $C_p$ are the density and heat capacity of the 10% PS-DEP solution, respectively. The unit of heat capacity is J/(g K). The heat capacity of the PS-DEP solution is estimated by a simple mixing rule [41]: $C_p = w_{PS} C_{p,PS} + w_{DEP} C_{p,DEP}$, where $w_{PS}$ and $w_{DEP}$ are the weight fractions of PS and DEP; $C_{p,PS}$ and $C_{p,DEP}$ are the heat capacities of PS and DEP, respectively. The values of $C_{p,PS}$ [0.93 J/(g K)] and $C_{p,DEP}$ [1.53 J/(g K)] at $-40\,^\circ$C are estimated from Refs. [36,42]. Therefore, with the amount of energy dissipation (see Fig. 8) in the present experiments, $\Delta T$ is approximately 2–7 mK, which is significantly smaller than that in the NSHB measurements. Also, here the stress_MSHB experiments were performed on the rubbery plateau which is well above the glass transition temperature, and material properties are insensitive to such small temperature change. Therefore, localized temperature changes are not expected to be the cause of the observed holes and the observed heterogeneity (holes) is attributed to the type of dynamics as postulated by Qin *et al.* [21].

### D. Hole refilling

The third effect investigated here is hole refilling, i.e., the effect of waiting time ($t_w$) between the pump modification
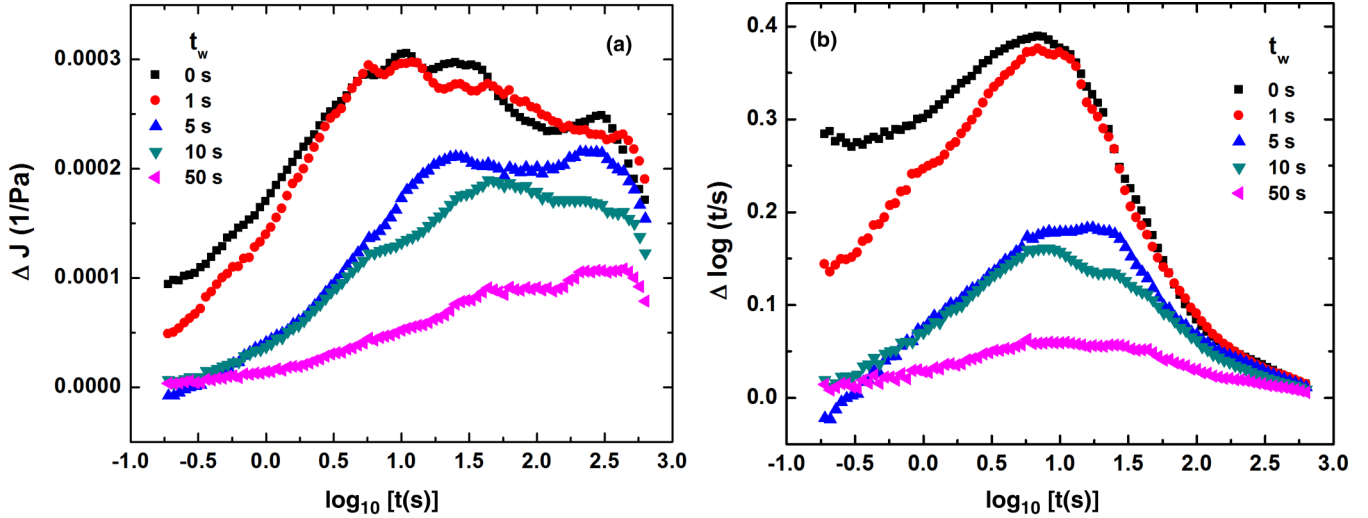
FIG. 10. The mechanical spectral modifications in (a) vertical direction and (b) horizontal direction for 10% PS-DEP solution at $-40\,^{\circ}$C as a function of waiting time between pump modification and probe stress. The pump stress amplitude, frequency, and probe stress are 2500 Pa, 0.05 Hz, and 25 Pa, respectively.

and probe. The pump stress amplitude, frequency, and probe stress are fixed at 2500 Pa, 0.05 Hz, and 25 Pa, respectively, while $t_w$ is varied from 0 to 50 s. Figure 10 plots the obtained mechanical modification in both directions. The hole intensity and position vary strongly with waiting time. When $t_w$ is small, i.e., 1 s, both the vertical hole and horizontal hole remain almost unchanged compared with 0 s waiting time. As $t_w$ increases, the intensity of the holes in both directions decreases. Such a hole intensity change shows a "fading memory" effect; i.e., the material forgets the previous pump modification with time. Moreover, as the waiting time increases, the position of the vertical hole shifts strongly to longer time, while the position of the horizontal hole only slightly shifts. Similar observation of hole refilling (hole intensity decreasing and hole position shifting) has been reported in the strain_MSHB [20] and NSHB experiments [4–6,8,10,14,15].

Figure 11 shows a double logarithmic plot of vertical hole intensity ($\Delta$J) vs waiting time ($t_w$), along with the fit of a KWW [1,2] function ($\Delta J_{\max}(t_w) = \Delta J_{\max}(0)\exp[-(t_w/\tau_{\text{refill}})^\beta]$) to the data. The characteristic hole refill time is $\tau_{\text{refill}} = 37.1$ s which is greater than the characteristic retardation time of 4.6 s from a KWW fit to the linear creep response, and much greater than the characteristic relaxation time of 0.0003 s from a KWW fit to the linear stress relaxation response. Such slow refilling reflects different recovery rates of subensembles in the response: The faster subensembles recover first; the slower ones recover over a longer time. As a result, the position of the holes shifts to longer time. Such slow hole refilling has been reported by Shi and McKenna in strain_MSHB measurements on polymeric materials [low density polyethylene (LDPE) melt and 30 wt% PS-DEP solution] [20]. In the case of studies using other types of stress-controlled hole burning technique, i.e., dielectric and magnetic NSHB, mixed results have been reported. The work on the supercooled liquids (propylene carbonate and glycerol) [4–6] and a supercooled plastic crystal (cyclo-octanol) [17] have shown much faster refilling process, where the timescale of hole refilling is similar to that of

the linear relaxation response; however, works in dielectric hole burning in relaxor ferroelectrics [14–16], binary organic glass formers [8], glycerol in the high frequency wing [9], $\beta$ relaxation of D-sorbitol [13], and magnetic hole burning on a spin glass [10] have reported the presence of such a slow hole refilling process. Such a response has been referred to as long-lived dynamic heterogeneity [14].

### E. Long-time peak

Referring back to Figs. 5(a), 7(a), and 10(a), we see in the vertical modification response a long-time peak at approximately $\log(t) = 2.5$. The intensity of the peak changes with pump stress amplitude, pump frequency, and waiting time.
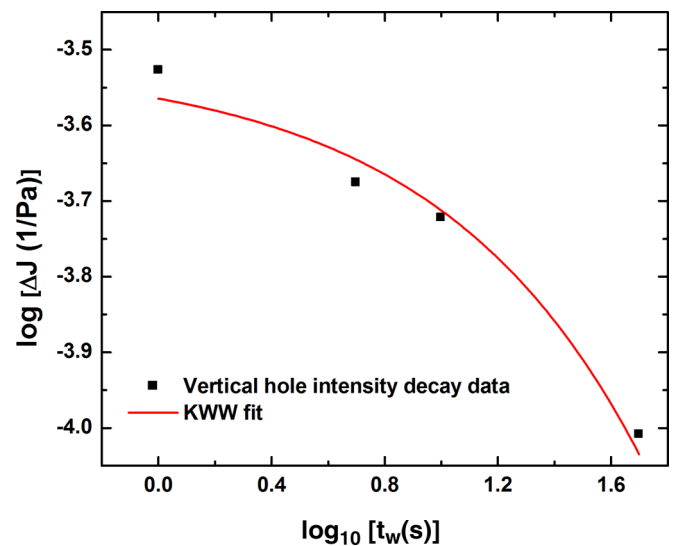


FIG. 11. Vertical hole intensity decay as a function of waiting time and fitted with a KWW function. The characteristic hole refill time $\tau_{\text{refill}}$ is 37.1 s and stretch parameter $\beta$ is 0.6.
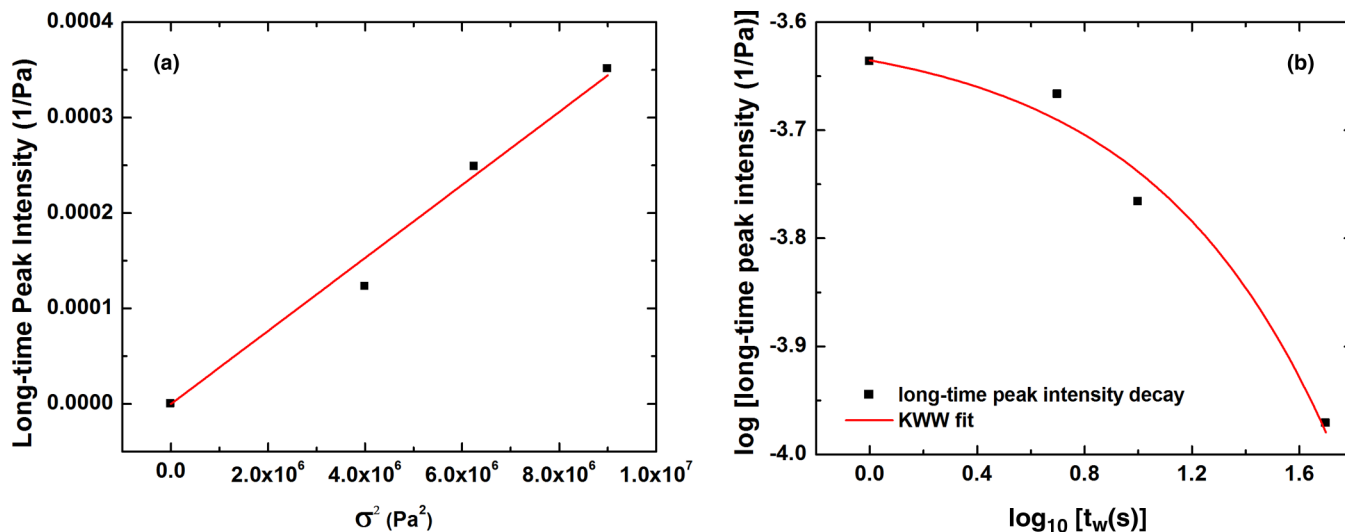
FIG. 12. (a) The intensity of long-time peak as a function of the square of pump stress amplitude and (b) the decay of long-time peak intensity with waiting time, fitted with a KWW function. The characteristic time $\tau$ is 62.9 s and stretch parameter $\beta$ is 0.64.

[For example, Fig. 12(a) shows the long-time peak intensity is proportional to the square of pump amplitude and Fig. 12(b) shows the intensity of long-time peak decays with waiting time, which is described with a KWW function with the characteristic time of 62.9 s and stretch parameter $\beta$ of 0.64.] However, the position of this peak is insensitive to pump parameters (stress amplitude and frequency) and waiting time, which is quite different from the behavior of vertical and horizontal holes. The origins of this peak are not clear and require further investigation.

## IV. CONCLUSIONS

In this work, the mechanical spectral hole burning (MSHB) technique has been extended from strain-controlled conditions (strain_MSHB) to stress-controlled conditions (stress_MSHB). The stress_MSHB technique has been applied to examine the behavior of a polymeric material, 10% PS-DEP solution. The effects of pump amplitude, pump frequency, and waiting time inserted between pump and probe on the development of nonresonant holes in the response have been discussed and compared with those obtained from strain_MSHB and other NSHB methods. Complete vertical and horizontal holes were burned in the system for all the effects investigated, which is slightly different from the strain_MSHB response of the same solution, for which only complete horizontal holes are obtained and vertical holes are only partially observed. In the current stress_MSHB test, a quadratic dependence of hole in-

tensity on pump amplitude is obtained, similar to observations in strain_MSHB and other hole burning techniques (dielectric and magnetic). Also, although the vertical hole intensity increases with the pump amplitude, its position is insensitive to the amplitude but depends on frequency, consistent with the nature of dynamic heterogeneity being frequency sensitive. Furthermore, the hole intensity has been shown to linearly increase with the dissipated energy due to the large stress pump. However, the estimates of induced temperature change are less than 10 mK which is insufficient to explain the appearance of the holes in terms of spatial heterogeneity in temperature or in heat capacity. This is different from the interpretation of dielectric and other hole burning spectroscopies near the glass transition or $\beta$ relaxation. The results suggest that stress-controlled MSHB can be combined with strain-controlled MSHB to build a more complete framework to investigate the dynamics of polymeric materials and are consistent with the dynamic heterogeneity being related to the type of dynamics rather than to localized heating effects. MSHB may also form the basis for future evaluations of nonlinear constitutive models [43].

[1] R. Kohlrausch, Theorie des elektrischen Rückstandes in der Leidener Flasche, Ann. Phys. **167**, 56 (1854).

[2] G. Williams and D. C. Watts, Non-symmetrical dielectric relaxation behaviour arising from a simple empirical decay function, Trans. Faraday. Soc. **66**, 80 (1970).

[3] R. Richert, Heterogeneous dynamics in liquids: Fluctuations in space and time, J. Phys.: Condens. Matter **14**, R703 (2002).

[4] B. Schiener, R. Böhmer, A. Loidl, and R. V. Chamberlin, Nonresonant spectral hole burning in the slow dielectric response of supercooled liquids, Science **274**, 752 (1996).

[5] B. Schiener, R. V. Chamberlin, G. Diezemann, and R. Böhmer, Nonresonant dielectric hole burning spectroscopy of super-cooled liquids, J. Chem. Phys. **107**, 7746 (1997).

[6] R. V. Chamberlin, B. Schiener, and R. Böhmer, Slow dielectric relaxation of supercooled liquids investigated by nonresonant spectral hole burning, Mater. Res. Soc. Symp. Proc. **455**, 117 (1997).

[7] K. R. Jeffrey, R. Richert, and K. Duvvuri, Dielectric hole burning: Signature of dielectric and thermal relaxation time heterogeneity, J. Chem. Phys. **119**, 6150 (2003).

[8] T. Blochowicz and E. A. Rossler, Nonresonant dielectric hole burning in neat and binary organic glass formers, J. Chem. Phys. **122**, 224511 (2005).

[9] K. Duvvuri and R. Richert, Dielectric hole burning in the high frequency wing of supercooled glycerol, J. Chem. Phys. **118**, 1356 (2003).

[10] R. V. Chamberlin, Nonresonant Spectral Hole Burning in a Spin Glass, Phys. Rev. Lett. **83**, 5134 (1999).

[11] R. Richert and R. Böhmer, Heterogeneous and Homogeneous Diffusivity in an Ion-Conducting Glass, Phys. Rev. Lett. **83**, 4337 (1999).

[12] R. Richert, The modulus of dielectric and conductive materials and its modification by high electric fields, J. Non-Cryst. Solids **305**, 29 (2002).

[13] R. Richert, Spectral selectivity in the slow $\beta$-relaxation of a molecular glass, Europhys. Lett. **54**, 767 (2001).

[14] O. Kircher, B. Schiener, and R. Böhmer, Long-Lived Dynamic Heterogeneity in a Relaxor Ferroelectric, Phys. Rev. Lett. **81**, 4520 (1998).

[15] O. Kircher, G. Diezemann, and R. Böhmer, Nonresonant dielectric hole-burning spectroscopy on a titanium-modified lead magnesium niobate ceramic, Phys. Rev. B **64**, 054103 (2001).

[16] T. El Goresy, O. Kircher, and R. Böhmer, Nonresonant hole burning spectroscopy of the relaxor ferroelectric PLZT, Solid State Commun. **121**, 485 (2002).

[17] R. Böhmer and G. Diezemann, Principles and applications of pulsed dielectric spectroscopy and nonresonant dielectric hole burning, in *Broadband Dielectric Spectroscopy*, edited by F. Kremer and A. Schönhals (Springer-Verlag, Berlin, Heidelberg, 2003).

[18] R. Richert, Dielectric hole burning in an electrical circuit analog of a dynamically heterogeneous system, Phys. A (Amsterdam, Neth.) **322**, 143 (2003).

[19] X. F. Shi and G. B. McKenna, Mechanical Hole Burning Spectroscopy: Evidence for Heterogeneous Dynamics in Polymer Systems, Phys. Rev. Lett. **94**, 157801 (2005).

[20] X. F. Shi and G. B. McKenna, Mechanical hole-burning spectroscopy: Demonstration of hole burning in the terminal relaxation regime, Phys. Rev. B **73**, 014203 (2006).

[21] Q. Qin, H. Doen, and G. B. McKenna, Mechanical spectral hole burning in polymer solutions, J. Polym. Sci., Part B: Polym. Phys. **47**, 2047 (2009).

[22] N. Shamim and G. B. McKenna, Mechanical spectral hole burning in polymer solutions: Comparison with large amplitude oscillatory shear fingerprinting, J. Rheol. **58**, 43 (2014).

[23] Q. Qin, X. F. Shi, and G. B. McKenna, Mechanical hole burning spectroscopy in an SIS tri-block copolymer, J. Polym. Sci., Part B: Polym. Phys. **45**, 3277 (2007).

[24] A. Deres, G. A. Floudas, K. Müllen, M. Van der Auweraer, F. De Schryver, J. Enderlein, H. Uji-i, and J. Hofkens, The origin of heterogeneity of polymer dynamics near the glass temperature as probed by defocused imaging, Macromolecules **44**, 9703 (2011).

[25] A. Kaye, Non-Newtonian flow of incompressible fluids, Report (College of Aeronautics Cranfield, Cranfield, UK, 1962).

[26] B. Berstein, E. A. Kearsley, and L. J. Zapas, A study of stress relaxation with finite strain, Trans. Soc. Rheol. **7**, 391 (1963).

[27] M. Doi and S. F. Edwards, Dynamics of concentrated polymer systems. Part 1.—Brownian motion in the equilibrium state, J. Chem. Soc., Faraday Trans. 2, **74**, 1789 (1978).

[28] M. Doi and S. F. Edwards, Dynamics of concentrated polymer systems. Part 2.—Molecular motion under flow, J. Chem. Soc., Faraday Trans. 2 **74**, 1802 (1978).

[29] M. Doi and S. F. Edwards, Dynamics of concentrated polymer systems. Part 3.—The constitutive equation, J. Chem. Soc., Faraday Trans. 2 **74**, 1818 (1978).

[30] M. Doi and S. F. Edwards, Dynamics of concentrated polymer systems. Part 4.—Rheological properties, J. Chem. Soc., Faraday Trans. 2 **75**, 38 (1979).

[31] M. Doi and S. F. Edwards, *The Theory of Polymer Dynamics* (Oxford Science Publishers, Oxford, 1986).

[32] A. Shokooh, Stress clock function in viscoelastic materials, Ph.D. thesis, Illinois Institute of Technology, 1977.

[33] B. Bernstein and A. Shokooh, The stress clock function in viscoelasticity, J. Rheol. **24**, 189 (1980).

[34] R. H. Ewoldt, A. E. Hosoi, and G. H. McKinley, New measures for characterizing nonlinear viscoelasticity in large amplitude oscillatory shear, J. Rheol. **52**, 1427 (2008).

[35] T. G. Fox, Bull. Am. Phys. Soc. **1**, 123 (1956), as cited in the Polymer Properties Database, http://polymerdatabase.com/polymer%20physics/Fox.html.

[36] S. S. Chang, J. A. Horman, and A. B. Bestul, Heat Capacities and related thermal data for diethyl phthalate crystal, glass and liquid to 360 °K, J. Res. Natl. Bur. Stand., Sect. A **71**, 293 (1967).

[37] J. D. Ferry, *Viscoelastic Properties of Polymers* (Wiley, New York, 1980).

[38] K. Hyun and M. Wilhelm, Establishing a new mechanical nonlinear coefficient $Q$ from FT-rheology: First investigation of entangled linear and comb polymer model systems, Macromolecules **42**, 411 (2009).

[39] D. S. Pearson and W. E. Rochefort, Behavior of concentrated polystyrene solutions in large-amplitude oscillating shear fields, J. Polym. Sci., Part B: Polym. Phys. **20**, 83 (1982).

[40] J. M. Dealy and K. F. Wissbrun, *Melt Rheology and Its Role in Plastics Processing: Theory and Applications*. (Kluwer Academic Publishers, Dordrecht, 1990).

[41] A. S. Teja, Simple method for the calculation of heat-capacities of liquid-mixtures, J. Chem. Eng. Data **28**, 83 (1983).

[42] U. Gaur and B. Wunderlich, Heat capacity and other thermodynamic properties of linear macromolecules. V. Polystyrene, J. Phys. Chem. Ref. Data **11**, 313 (1982).

[43] X. Shi, Rheology of complex fluids: Mechanical hole burning spectroscopy and organic complex fluids, Ph.D. dissertation, Texas Tech University, 2004; https://www.ttu-ir.tdl.org/ttu-ir/handle/2346/11538.